Manupulating Proton Transfer Process in Molecular Complexes: Synthesis and Spectroscopic Studies

Sumit Kumar Panja, Nidhi Dwivedi, and Satyen Saha*

Department of Chemistry, Centre for Advanced Studies, Institute of Science, Banaras Hindu University, Varanasi-221005, India

Synthetic Procedures for Molecular Complex

N-methylpiperidine (1.01 mmol) was taken in 50 ml round bottom flask containing 5 ml $CHCl_3$ and nitrophenol derivative (1 mmole) was added. Immediate yellowish coloured liquid was obtained. Resulting yellowish solution was stirred for 1-2 h at room temperature and was kept in refrigerator. Finally yellow colour crystal was separated out from solvent. After detailed analysis, we found that 1:2 stoichiometric molecular complex for 4-nitrophenol with N-methylpiperidine whereas 1:1 stoichiomeric molar complex for 2,4-dinitrophenol and 2,4,6-trinitrophenol with N-methylpiperidine.

Analytical data for [MP(NP)$_2$]: $C_{18}H_{23}N_3O_6$ Complex: C, 58.25 % (58.20 %); H, 6.20 % (6.16 %); N, 10.65 % (10.63 %); M.P.:63.2 ˚C; ^{1}H NMR (300 MHz, $CDCl_3$) :δ(ppm) 8.12 (d, *J* = 9 Hz, 4H), 6.80 (d, *J* = 9 Hz, 4H); 5.13 (broad, 1H), 2.81 (t, *J* = 8.1 Hz, 4H), 2.55 (s, 3H); 1.83-1.76 (m, 4H), 1.60-1.52 (m, 2H); ^{13}C-NMR (75 MHz, $CDCl_3$):δ (ppm) 165.8, 139.5, 126.5, 116.5, 55.6, 45.0, 23.8, 22.2.

Analytical data for [MP(DNP)]:$C_{12}H_{17}N_3O_5$ Complex: C, 50.88 % (58.80 %); H, 6.05 % (6.00 %); N, 14.83 % (14.80 %); M.P.:143.2˚C; ^{1}H-NMR (300 MHz, $CDCl_3$) :δ (ppm) 8.99 (s, 1H), 8.06 (d, *J* = 9.6 Hz, 1H), 6.69 (d, *J* = 9.3 Hz, 1H), 3.23 (broad, 1H), 3.17-3.02 (broad, 4H), 2.77 (broad, 3H), 1.93-1.87 (broad, 4H), 1.67-1.58 (broad, 2H); ^{13}C-NMR (75 MHz, $CDCl_3$):δ (ppm) 170.3, 135.2, 132.1, 128.9, 126.7, 125.2, 55.6, 44.3, 22.9, 21.5.

Analytical data for [MP(TNP)]:$C_{12}H_{17}N_3O_5$ complex: C, 43.90 % (43.80 %); H, 4.91 % (5.00 %); N, 17.17 % (18.00 %); M.P.:226.6 ˚C; ^{1}H-NMR (300 MHz, $CDCl_3$) :δ (ppm) 8.88(s, 1H), 3.66 (broad, 1H), 2.86-2.02 (broad, 7H), 1.9 (broad, 4H), 1.93 (broad, 2H); ^{13}CNMR (75 MHz, $CDCl_3$): δ (ppm) 162.0, 141.63, 128.1, 126.5, 55.9, 44.5, 22.8, 21.4.

Conformational Analysis

Theoretically we have also calculated energy of the conformational changes of protonated piperidium cation from conformer I to conformer II. It is observed that the conformational energy is ~2.4 kcalmol^{-1} i.e. easity available at room temperature condition.

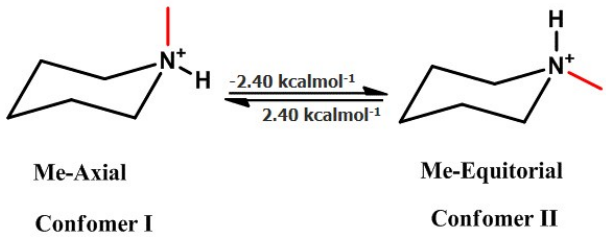

Figure 1. Conformational change between me-Axial and me-equatorial of protonated (NPH^+) from DFT calculation

Thermo gravimetric analysis (TGA)

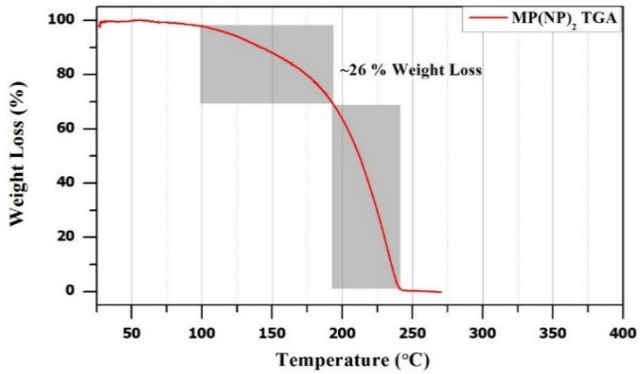

Figure 2: TGA Plots of $MP(NP)_2$ Molecular Complex

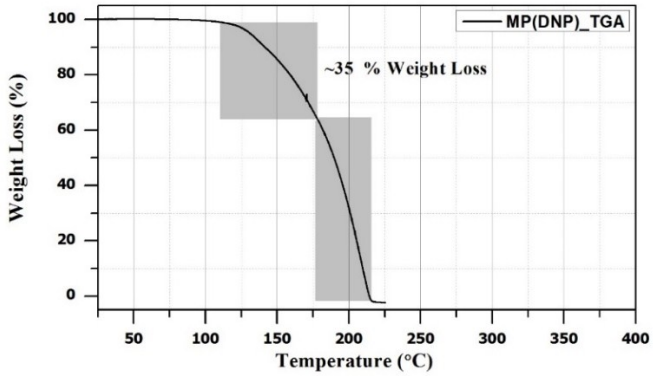

Figure 3: TGA Plots of MP(DNP) Molecular Complex

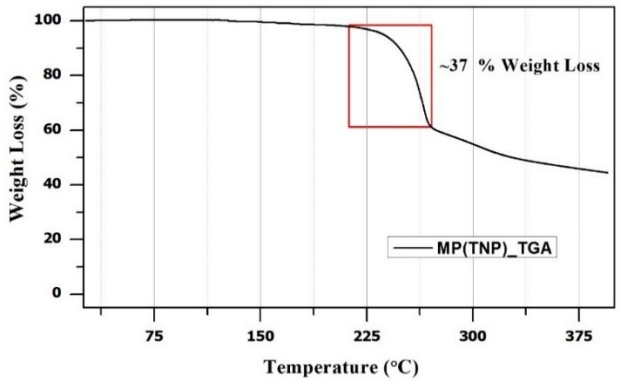

Figure 4: TGA Plots of MP(TNP) Molecular Complex

Single Crystal X-ray Diffraction

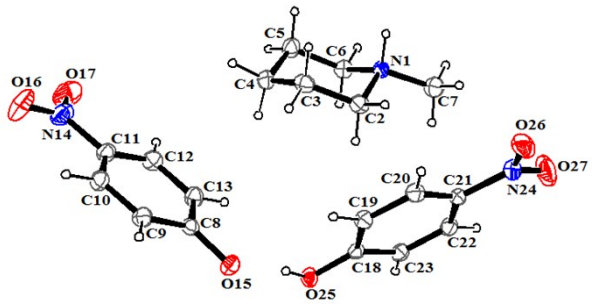

Figure 5: ORTEP diagram of MP(NP)2 (**CCDC** No.: **881652**)

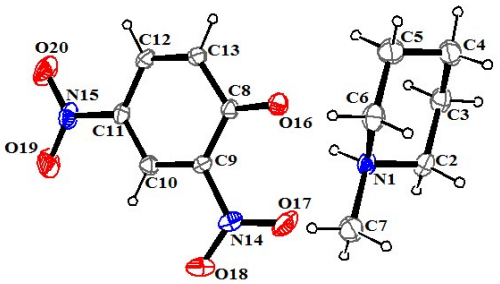

Figure 6: ORTEP diagram of MP(DNP) (**CCDC** No.: **873550**).

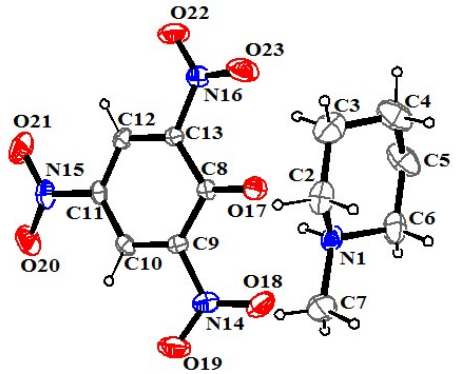

Figure 7: ORTEP diagram of MP(TNP) (**CCDC** No.: **917775**).

Table 1: Crystallographic data

Compound	$MP(NP)_2$	MP(DNP)	MP(TNP)
Formula	$C_{18}H_{23}N_3O_6$	$C_{12}H_{17}N_3O_5$	$C_{12}H_{16}N_4O_7$
Fw	377.39	283.29	328.29
a (Å)	6.5076(3)	7.5357(6)	7.123(5)
b (Å)	7.9798(6)	17.1542(11)	20.470(5)
c (Å)	18.3407(14)	10.8286(9)	10.498(5)
α (°)	90.054(6)	90	90
β (°)	92.065(5)	102.802(9)	93.020(5)
γ (°)	98.928(5)	90	90
V (Å^3)	940.25(11)	319.54(5)	1528.6(13)
Z	2	4	4
space group	P-1	P21/c	P21/n
D_{calcd} (g cm^{-3})	1.333	1.378	1.427
R (F_o^2)[a]	0.0523	0.0570	0.0583
$R_w(F_o^2)$[b]	0.1095	0.1282	0.1393

$^{a}R = \Sigma\|\|F_o\| - \|F_c\|\|/\Sigma\|F_o\|$ $^{b}R_w = [\Sigma w(F_o^2 - F_c^2)^2/ \Sigma w(F_o^4)]^{1/2}$

Table 2: Hydrogen bond lengths (Å) and angles (^{O}) of $MP(NP)_2$

D-H…A	d(D-H)	d(H..A)	<DHA	d(D..A)
C2-H2A...O26#1	0.970	2.462	139.39	3.260
C3-H3A...O15#2	0.970	2.611	167.81	3.565
C7-H7B...O26#1	0.960	2.535	138.91	3.319
C23-H23...O15#3	0.930	2.648	151.91	3.496
O25-H25...O15	0.820	1.701	172.47	2.516
N1-H1...O25#2	0.953	1.811	171.68	2.758

Symmetry transformations used to generate equivalent atoms: #1 -x, -y+3, -z; #2 x, y+1, z; #3 x-1, y, z;

Table 3: Hydrogen bond lengths (Å) and angles (^{O}) of MP(DNP)

D-H…A	d(D-H)	d(H..A)	<DHA	d(D..A)
C7-H7A...O19#1	0.960	2.536	151.86	3.413
C7-H7B...O17	0.960	2.354	122.47	2.982
C7-H7C...O18#2	0.960	2.504	138.08	3.282
N1-H1...O16	0.909	1.821	164.86	2.709
N1-H1...O17	0.909	2.517	119.45	3.068

Symmetry transformations used to generate equivalent atoms: #1 -x, -y+1, -z+1; #2 x, -y+3/2, z-1/2.

Table 4: Hydrogen bond lengths (Å) and angles (^{O}) of MP(TNP)

D-H…A	d(D-H)	d(H..A)	<DHA	d(D..A)
C7-H7A...O21#1	0.960	2.612	147.12	3.457
C7-H7B...O18	0.960	2.574	123.99	3.211
N1-H1...O17	0.902	1.852	165.49	2.735

Symmetry transformations used to generate equivalent atoms: #1 -x+1, -y, -z+2.

FTIR Spectra of Molecular Complexes

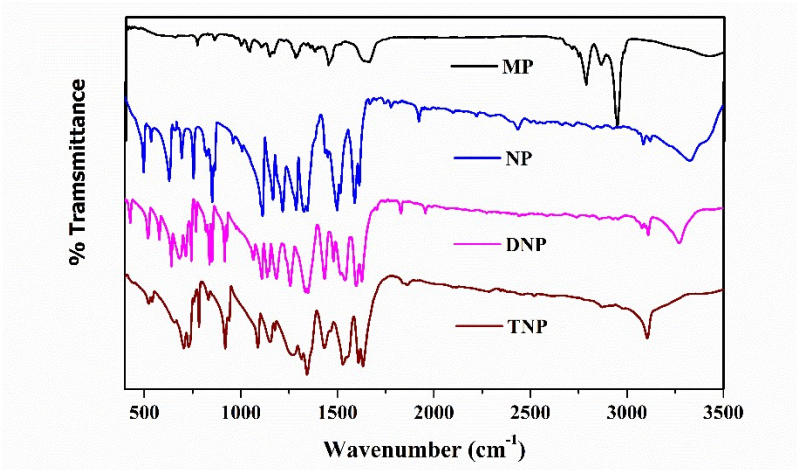

Figure 8: FTIR Spectra of MP, NP, DNP and TNP

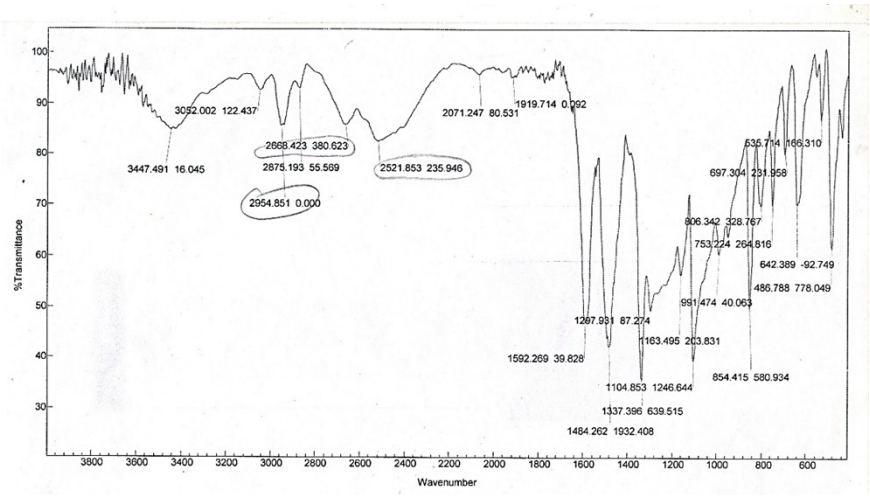

Figure 9: FTIR Spectra of $MP(NP)_2$

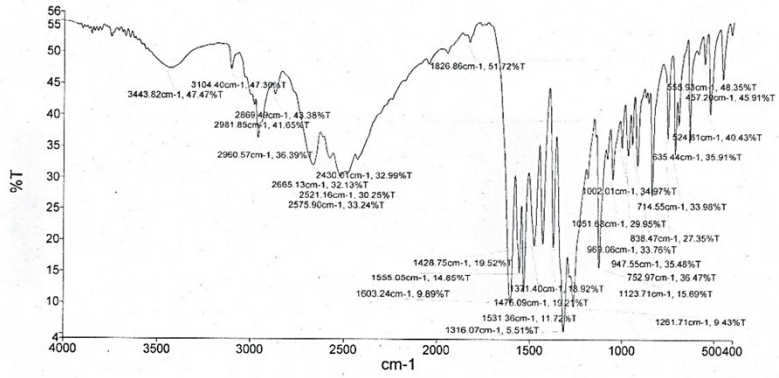

Figure 10: FTIR Spectra of MP(DNP)

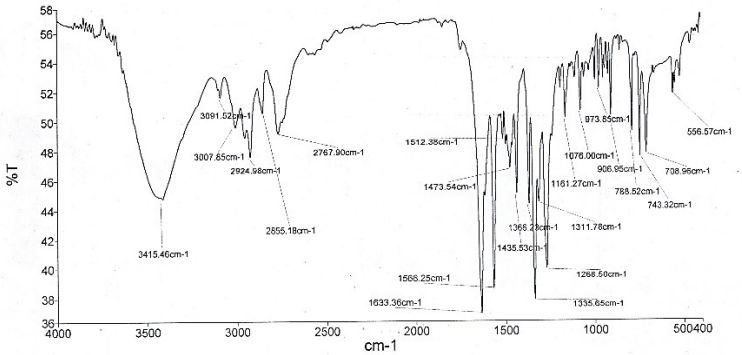

Figure 11: FTIR Spectra of MP(TNP)

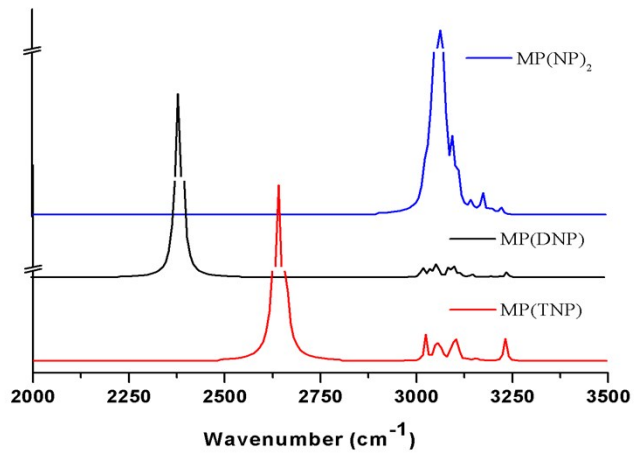

Figure 12: Theoretical FTIR Spectra of all three molecular Complexes

Stoichiomery of Molecular Complexes by Job's Method

Job's plot of $MP(NP)_2$ in ACN at 420 nm

A series of solutions containing MP and NP were prepared such that sum of total number of mole MP and NP concentration remained constant ($1x10^{-3}$(M). The mole fraction (X) of MP was varied from 0.1 to 1.0. The corrected absorbance (OD_{420} x X_{MP} $x10^{-3}$) at 420 nm was plotted against the molar fraction of the MP.

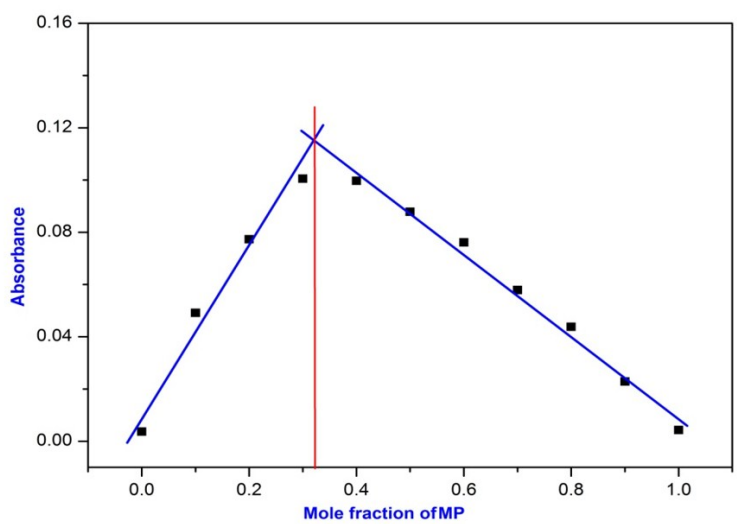

Figure 13: Job's plot of $MP(NP)_2$ in ACN at 420 nm.

Job's plot of MP(DNP) in ACN at 425 nm

A series of solutions containing MP and DNP were prepared such that the sum of the total number of mole MP and DNP concentration remained constant ($1x10^{-3}$(M). The mole fraction (X) of MP

was varied from 0.1 to 1.0. The corrected absorbance (OD_{425} x X_{MP} x10^{-3}) at 425 nm was plotted against the molar fraction of the MP solution.

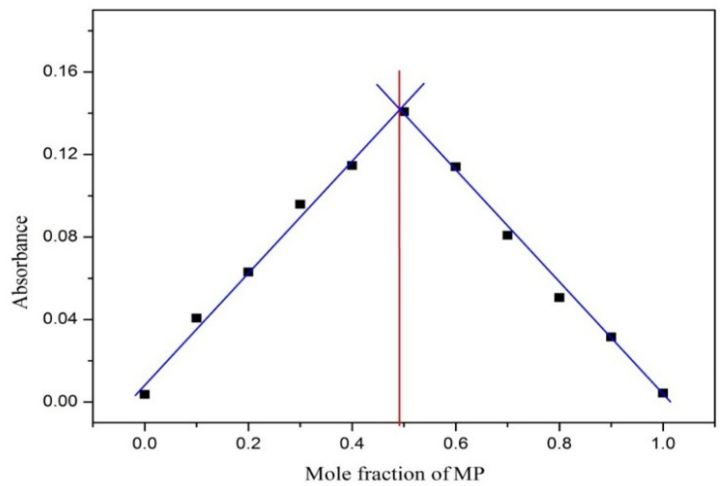

Figure 14: Job's plot of MP(DNP) in ACN at 425 nm.

Job's plot of MP(TNP) in ACN at 429 nm

A series of solutions containing MP and TNP were prepared such that the sum of the total number of mole MP and TNP concentration remained constant (1x10^{-4}(M). The mole fraction (X) of MP was varied from 0.1 to 1.0. The corrected absorbance (OD_{429} x X_{NMP} x10^{-4}) at 429 nm was plotted against the molar fraction of the MP solution.

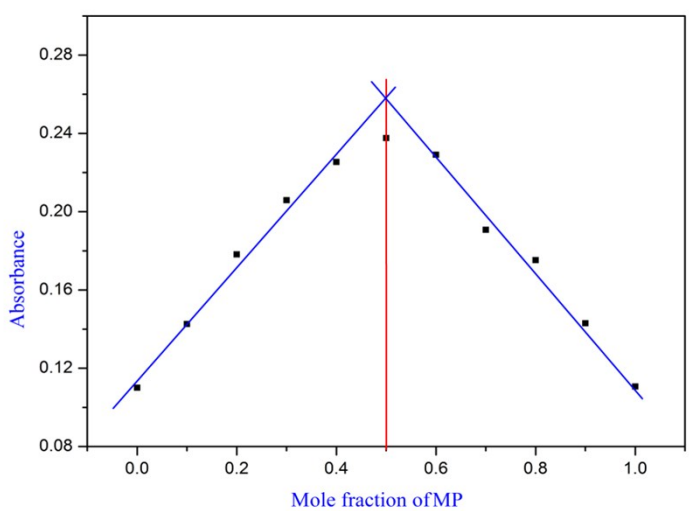

Figure 15: Job's plot of MP(TNP) in ACN at 429 nm.

Table 5: λ_{max} and molar Absorption Coefficients of ICT band in ACN

X of MPX	λ_{max}/nm	E_{CT}	$\varepsilon(\lambda_{max})$/moldm^{-3}cm^{-1}

		(eV)	
$MP(NP)_2$	419	2.96	737
MP(DNP)	425	2.92	2262
MP(TNP)	429	2.89	7392

Calculation of Association Constant by Benesi-Hildebrand Method

Benesi-Hildebrand Plot of $MP(NP)_2$ Formation in ACN at 420 nm.

Stoichiometry and the formation constant of molecular complex in acetonitrile have been investigated exclusively using Benesi-Hildebrand equation. The spectrophotometric titration was employed for calculation of formation constant (K_A) of the molecular complex. The change in absorbance upon addition of MP to a solution of NP of fixed concentration is measured. The Benesi-Hildebrand equation is the following form for 1:2 stoichiometric systems.

$$\frac{1}{[A - A_0]} = \frac{1}{K_{ICT}([A_{max} - A_0])[MP]2} + \frac{1}{[A_{max} - A_0]} \quad 1$$

Where, [MP] is the concentrations of MP (donor) and A is absorbance upon addition of MP. A_0 is the absorbance of NP (proton donor) in absence of MP (proton acceptor) at λ_{CT} against the solvent as reference

The 1:2 donor-acceptor interactions was analyzed according to Benesi-Hildebrand equations for spectroscopic UV-Vis titration.

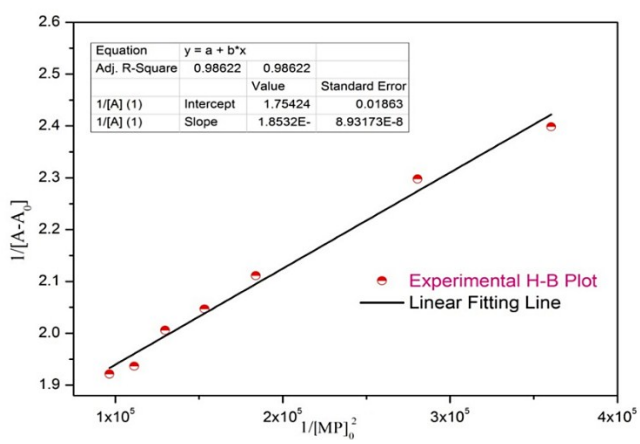

Figure 16: H-B plot of $MP(NP)_2$ molecular complex formation in acetonitrile solvent. Absorbance was monitored at 419 nm.

Table 5: B-H plot of $MP(NP)_2$ in ACN at 420 nm

Parameters	Intercept	Slope	Association Constant (K_A)	Stoichiometry

Linear Plot	1.75424	1.85×10^{-6}	9.4×10^{5} (M^{-2})	1:2

Benesi-Hildebrand plot of MP(DNP) formation in ACN at 425 nm.

Stoichiometry and the formation constant (K_A) of MP(DNP) in acetonitrile solvent at room temperature have been investigated exclusively using Benesi-Hildebrand equation. The spectrophotometric titration was employed for calculation of formation constant (K_A) of the complex. The change in absorbance upon addition of MP to a solution of DNP of fixed concentration is measure. The Benesi-Hildebrand equation is the following form for 1:1 stoichiometric system.

$$\frac{1}{[A - A_0]} = \frac{1}{K_{CT}([A_{max} - A_0])[MP]} + \frac{1}{[A_{max} - A_0]} \quad \ldots\ldots\ldots\ldots\ldots\ldots 2$$

Where, [MP] is the concentrations of MP (proton acceptor) and A is absorbance upon addition of MP. A_0 is the absorbance of DNP (proton donor) in absence of MP (donor) at λ_{CT} against the solvent as reference.

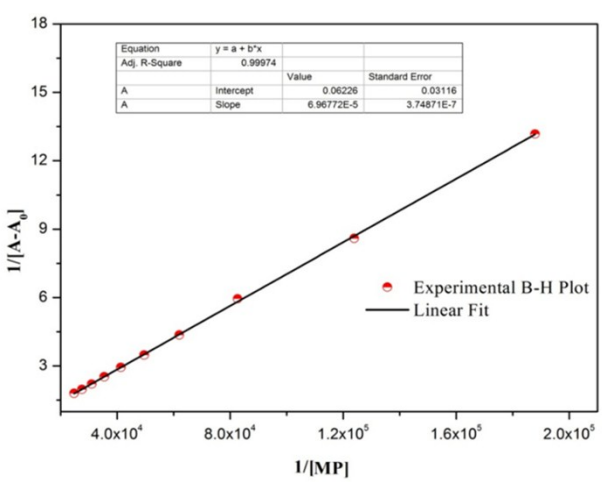

Figure 17: H-B plot of MP(DNP) in ACN at 425 nm.

The 1:1 donor-acceptor interactions was analysed according to Benesi-Hildebrand equations for spectroscopic UV-Vis titration

Table 6: B-H plot of MP(DNP) in ACN at 425 nm

Parameters	Intercept	Slope	Association Constant (K_A)	Stoichiometry

Linear Plot	0.06226	6.9677×10^{-5}	8.93×10^{2} (M^{-1})	1:1

Benesi-Hildebrand plot plot of $MP(TNP)_2$ formation in ACN at 429 nm

Stoichiometry and the formation constant (K_A) of MP(TNP) in ACN have been investigated exclusively using Benesi-Hildebrand equation. The spectrophotometric titration was employed for calculation of formation constant (K_A) of the complex. The change in absorbance upon addition of MP to a solution of TNP of fixed concentration is measured. The Benesi-Hildebrand equation is the following form for 1:1 stoichiometric system.

$$\frac{1}{[A - A_0]} = \frac{1}{K_{ICT}([A_{max} - A_0])[MP]} + \frac{1}{[A_{max} - A_0]} \quad \ldots\ldots\ldots\ldots\ldots\ldots 2$$

Where, [MP] is the concentrations of MP (donor) and A is absorbance upon addition of NMP. A_0 is the absorbance of TNP (proton donor) in absence of MP (proton acceptor) at λ_{CT} against the solvent as reference

The 1:1 donor-acceptor interactions was analyzed according to Benesi-Hildebrand equations for spectroscopic UV-Vis titration.

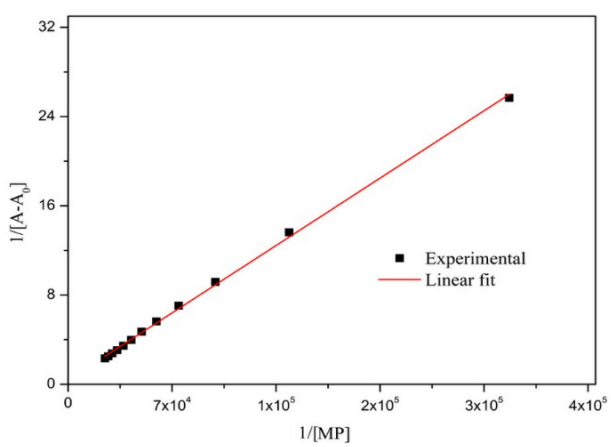

Figure 18: H-B plot of MP(TNP) in ACN at 429 nm (Deconvoluted spectra).

Table 7: B-H plot of MP(TNP) in ACN at 425 nm

Parameters	Intercept	Slope	Association Constant (K_A)	Stoichiometry
Linear Plot	0.36036	8.6291×10^{-5}	4.176×10^{3} (M^{-1})	1:1

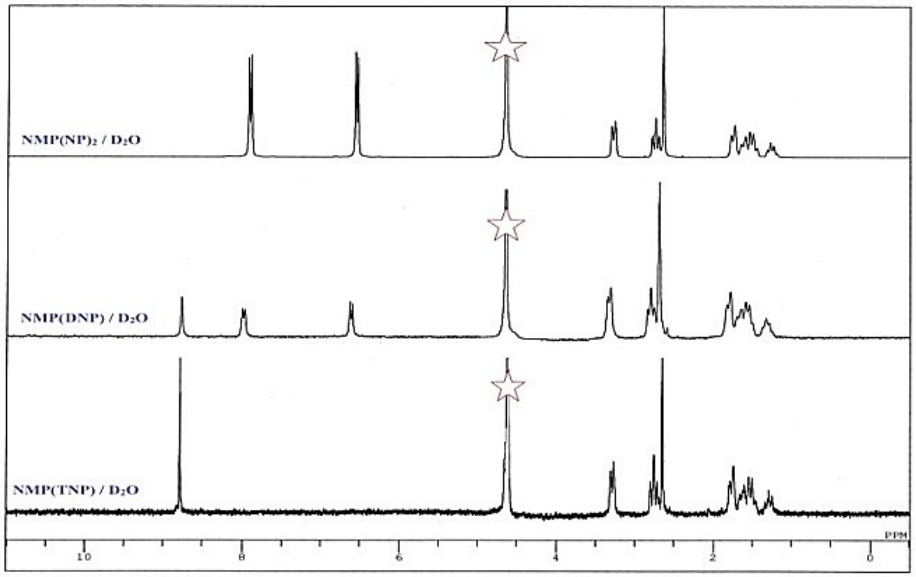

Figure 19: ^{1}H-NMR spectra of $MP(NP)_2$, MP(DNP) and MP(TNP) in D_2O (* due to the solvent)

Quantum Chemical Calculation

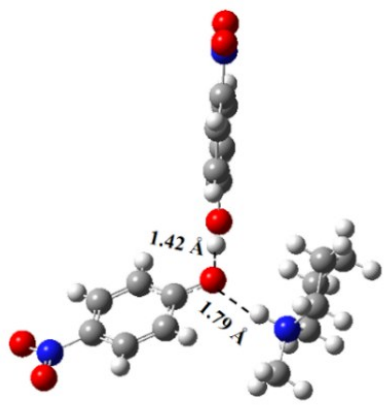

Figure 20a: Optimized Structure of $MP(NP)_2$

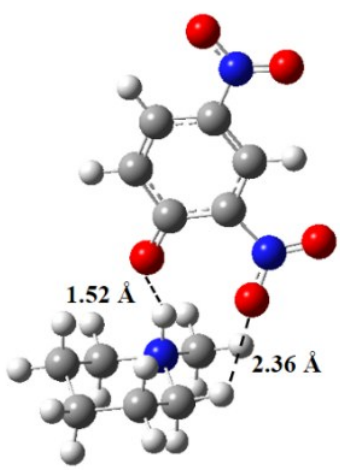

Figure 20b: Optimized Structure of MP(DNP)

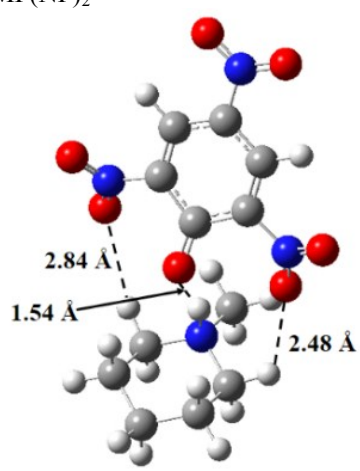

Figure 20c: Optimized Structure of MP(TNP)

Table 8: Bond angle, bond length and inter nuclear distance from DFT results

	SCXRD	DFT Result	SCXRD	DFT Result	SCXRD	DFT Result	XRD	DFT
	Angle of NHO		OH bond Length (A)		C-O bond Length		Inter nuclear distance (R)	
$MP(NP)_2$	170.17	165.02	1.80 0.92	0.97 0.96	1.31 1.33	1.35 1.37	2.76 2.51	2.53 2.60
MP(DNP)	164.96	158.92	1.82	1.52	1.25	1.26	2.70	2.56
MP(TNP)	167.29	163.11	1.84	1.54	1.23	1.25	2.73	2.59

Table 9: HOMO, LUMO diagram and their corresponding energy

$MP(NP)_2$		
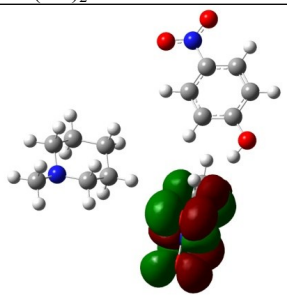 LUMO (-2.8795 eV)	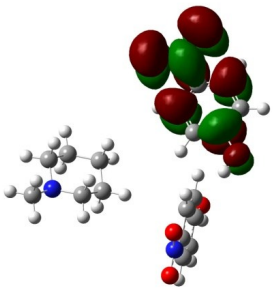 LUMO (+1)(-2.8795 eV)	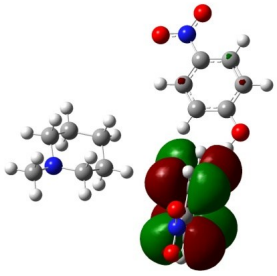 LUMO (+2) (-1.22508 eV)
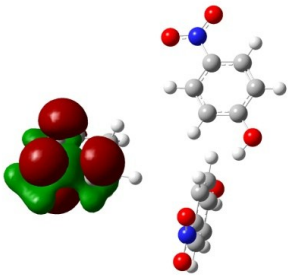 HOMO (eV) (-6.02745 eV)	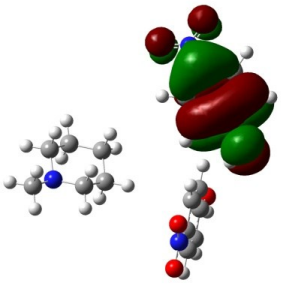 HOMO (-1) (-7.05743 eV)	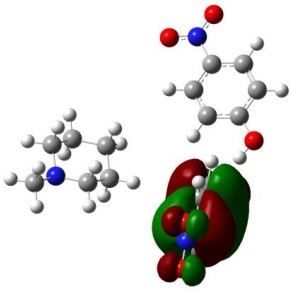 HOMO (-2) (-7.3741 eV)
NMP(DNP)		

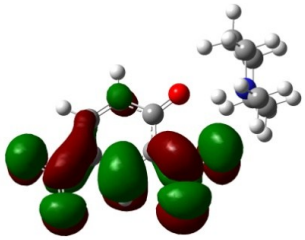 LUMO(-2.9122 eV)	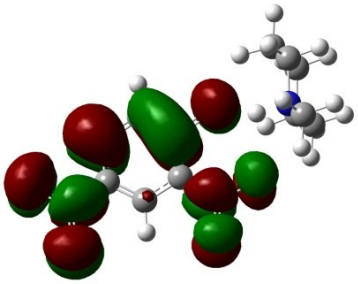 LUMO(+1)(-2.5475 eV)	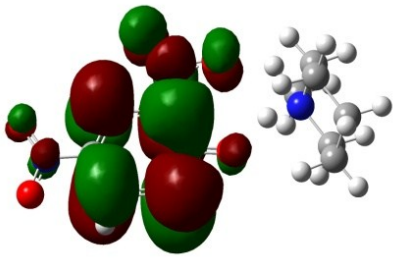 LUMO(+2)(-0.5053 eV)
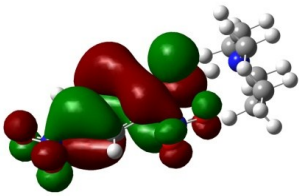 HOMO (-6.5572 eV)	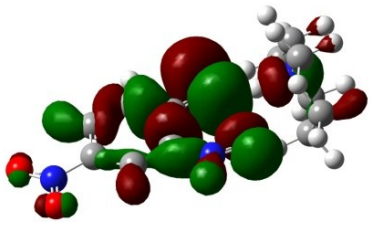 HOMO(-1)(-7.3856 eV)	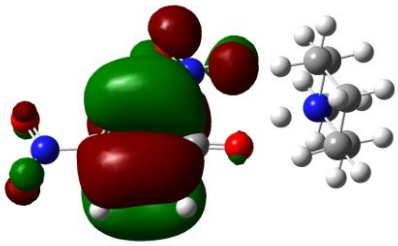 HOMO(-2)(-7.9712 eV)
MP(TNP)		
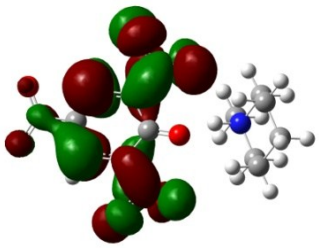 LUMO(-3.1348 eV)	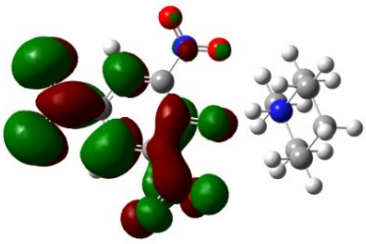 LU MO(+1)(-2.9239 eV)	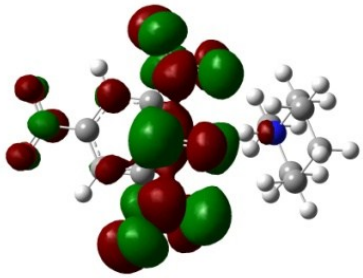 LUMO(+2)(-2.6681 eV)
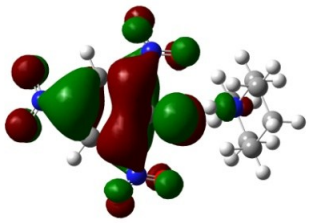 HOMO (-6.9534 eV)	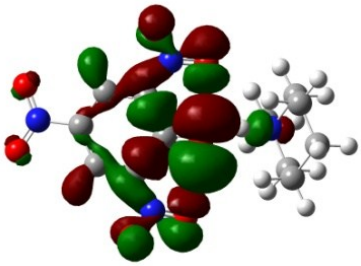 HOMO (-1) (-7.7121 eV)	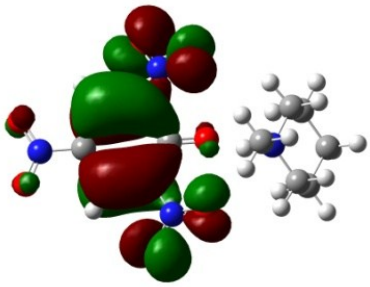 HOMO (-2) (-8.1497 eV)

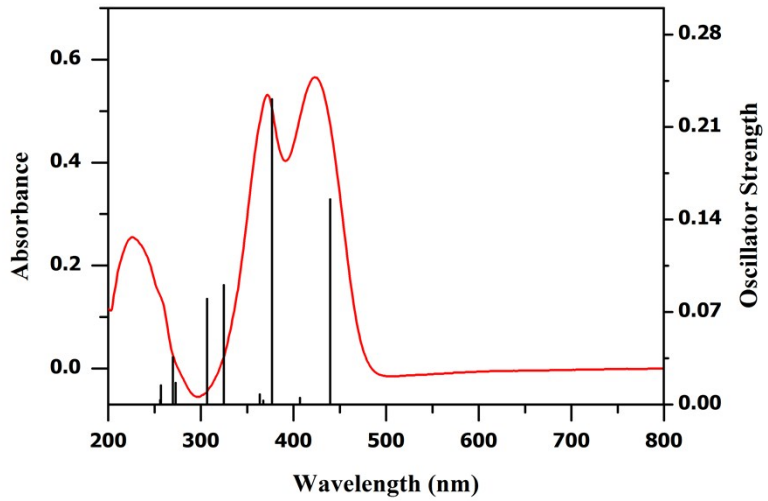

Figure 21: UV-Vis (experimental) and TD-DFT plot of MP(DNP)

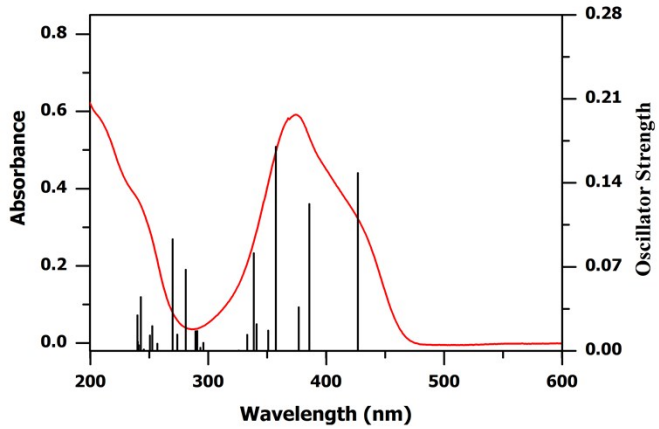

Figure 22: UV-Vis (experimental) and TD-DFT plot of MP(TNP)

Reference

1. (a) Benesi, H. A.; Hildebrand, J. H. *J. Am. Chem. Soc*. **1949**, 71, 2703; (b) Yang, C.; Liu, L.; Mu, T.-W.; Guo, Q.-X. *Anal. Sci*. **2000**, 16, 537; (c) Rodrıiguez-Caceres, M. I.; Agbaria, R. A.; Warner, I. M. *J. Fluoresc*., **2005**, 15, 185.
2. Sedo, G.; Leopold, K. R. Partial Proton Transfer in a Molecular Complex: Assessments from Both the Donor and Acceptor Points of View. *J. Phys. Chem*. A **2011**, 115, 1787-1794.
3. Koeppe, B.; Tolstoy, P. M.; Limbach, H. –H.; J. *Am. Chem. Soc*. **2011**, 133, 7897–7908.

4. (a) Libus, W.; Mecik, M.; Sulek, W. *J. Sol. Chem*. 1977, 6, 865; (b) Aono, S.; Kato, S. *J. Comp. Chem.* **2010,** 31, 2924-31; (c) Foster, R. *J. Phys. Chem*. **1980**, 84, 2135; (d) S. Nagakuara, S.; Gouterman, M. *J. Chem. Phys*. **1957**, 26, 881; (e) Al-Ahmary, K. M.; Habeeb, M. M.; Al-Solmy, E. A. *J. Molecu. Liquids*, **2011**, 158, 161.